Ocean Engineering 138 (2017) 151–160

Contents lists available at ScienceDirect

Ocean Engineering

journal homepage: www.elsevier.com/locate/oceaneng

Navigation vector based ship maneuvering prediction☆

Lokukaluge P. Perera

SINTEF Ocean (former MARINTEK), Trondheim, Norway

ARTICLE INFO

Keywords:
Maneuvering prediction
Ship predictor
Ship navigation
Inertial navigation systems
Marine vehicle detection and tracking

ABSTRACT

A novel mathematical framework for predicting ship maneuvers within a short time interval is presented in this study. The first part of this study consists of estimating the required vessel states and parameters by considering a kinematic vessel maneuvering model. That is supported by an extended Kalman filter (EKF), where vessel position, heading, yaw rate and acceleration measurements are used. Then, the estimated vessel states and parameters are used to derive the respective navigation vectors that consist of the pivot point information. The second part of this study consists of predicting the future vessel position and orientation (i.e. heading) within a short time interval by a vector product based algorithm, where the respective navigation vectors are used. The main advantage in this method is that the proposed framework can accommodate external environmental conditions and that feature improves the predictability of vessel maneuvers. Finally, the proposed mathematical framework is simulated and successful computational results in predicting ship maneuvers are presented in this study. Therefore, that can be implemented in modern integrated bridge systems to improve the navigation safety in maritime transportation.

1. Introduction

1.1. Ship maneuvers

Ship maneuvers may consist of complex vessel motions due to various external environmental conditions in the navigation area, i.e. wind and waves, ocean and tidal current conditions, riverbanks, water depth levels and other vessels. Hence, navigators often encounter decision making difficulties due to unpredictable ship behavior and underactuated vessel control systems (i.e. under conventional rudder-propeller-thruster control systems). Furthermore, combinations of such environmental conditions, i.e. draft variations in a passage from fresh to sea water with other vessels in the vicinity of the same navigation area, not only create additional navigation difficulties but also compromise the navigation safety. Similarly, ships under harbor maneuvers (i.e. in confined waterways) can encounter similar challenges, where each port may consist of an analogous set of local berthing criteria and that can create additional time consuming and potentially dangerous navigation situations (Brown et al., 1994). In general, navigator's knowledge and experience (i.e. with trial and error procedures) should extensively be used to overcome such critical situations, therefore the ship navigator should have adequate knowledge and experience to predict vessel behavior and control speed, course and heading conditions, appropriately. Furthermore, appropriate vessel tracking and trajectory prediction tools (i.e. navigation aids) should be available under integrated bridge systems as decision support facilities to overcome the same challenges in shipping (Pathirana et al., 2004).

In general, nonlinear ship steering conditions cause such maneuvering difficulties (Perera and Soares, 2012) and increase the risk of collision among vessels in coastal and harbor navigation situations resulted in environmental disasters (Ministry of Infrastructures and Transports, 2012). Furthermore, additional time delays (i.e. to the navigators' actions) in vessel responses can further increase the risk of collision and grounding even under advanced steering and speed control systems (Perera et al., 2014a). Even though maneuvering prediction and collision avoidance systems are extensively developed and used under air and land transportation (Divelbiss and Wen, 1997), such navigation aids are still underdeveloped in maritime transportation. Therefore, this study proposes to develop the required navigation tools (Paley et al., 2008; Perera et al., 2014b) to predict ship maneuvers in maritime transportation and that can be implemented under integrated bridge systems.

The navigation tools developed to predict the behavior of vessels/vehicles are often associated with various mathematical models and estimation algorithms. However, nonlinear hydrodynamic forces and moments and their interactions in ship navigation can complicate such kinematic and dynamic models of ocean going vessels. Other than

☆ Manuscript received January 12th, 2016. An initial version of this paper is presented at the 10th IFAC Conference on Manoeuvring and Control of Marine Craft (MCMC'2015), Copenhagen, Denmark.

E-mail address: prasad.perera@sintef.no.

http://dx.doi.org/10.1016/j.oceaneng.2017.04.017
Received 23 November 2016; Received in revised form 14 April 2017; Accepted 15 April 2017
Available online 25 April 2017

Nomenclature

$\alpha(k)$ a scale factor.
$\beta(k)$ a scale factor.
δt a short time interval
$\mu(k)$ the angle between $B_{cg}(k)$ & $B_{ch}(k)$ (i.e. the same as $B_{cp}(k)$ & $B_{cq}(k)$)
$\chi(t)$ the course for the vessel
$\psi(t)$ the heading of the vessel
$\Omega(k)$ the yaw rate vector of the vessel
$a_{ng}(t)$ & $a_{tg}(t)$ the normal and tangential acceleration components of P_g
$a_{xg}(t)$ & $a_{yg}(t)$ the X & Y acceleration components of P_g
$a_u(t)$ & $a_v(t)$ the surge & sway acceleration components at P_g
$B_a(k)$ the estimated bearing vector of P_a with respect to P_o
$B_{cg}(k)$ the estimated bearing vector of P_g with respect to P_c
$B_{ch}(k)$ the estimated bearing vector of P_h with respect to P_c
$B_{cp}(k)$ the estimated bearing vector of P_p with respect to P_c
$B_{cq}(k)$ the estimated bearing vector of P_q with respect to P_c
$B_g(k)$ the estimated bearing vector of P_g with respect to P_o
$B_{ga}(k)$ the estimated bearing vector of P_a with respect to P_g
$B_{gp}(k)$ the estimated bearing vector of P_p with respect to P_g
$B_h(k)$ the estimated bearing vector of P_h with respect to P_o
$B_{hq}(k)$ the estimated heading vector of the future vessel position
$B_p(k)$ the estimated bearing vector of P_p with respect to P_o
$B_q(k)$ the estimated bearing vector of P_q with respect to P_o
$f(.)$ the system function matrix
$h(.)$ the measurement function matrix
k the discreet-time instant of each parameter
l_{xp} & l_{yp} the X & Y distances from P_g to P_p
P_a a general point located along the centerline of the vessel
P_c the center of planar motion of the vessel
P_g the current center of gravity of the vessel (i.e. the current vessel position)
P_h the center of gravity of the future vessel position
P_o the origin of XYZ coordinate system
P_p the current pivot point of the vessel
P_q the pivot point of the future vessel position
$Q(t)$ the covariance matrix of system noise
$R(t)$ the covariance matrix of measurement noise
$R_p(k)$ the magnitude of $B_{cp}(k)$
$R_g(k)$ the magnitude of $B_{cg}(k)$
$r(t)$ the yaw rate of the vessel
t the continuous-time instant of each parameter
$u(t)$ & $v(t)$ the surge and sway velocity component of P_g
$V(t)$ the course-speed vector of the vessel
$V_a(t)$ the velocity vector at P_a
$v_{xa}(t)$ & $v_{ya}(t)$ the X & Y velocity components of P_a
$v_{ua}(t)$ & $v_{va}(t)$ the surge and sway velocity components of P_a
$v_{xg}(t)$ & $v_{yg}(t)$ the X & Y velocity components of P_g
$w_g(t)$ the white Gaussian system noise matrix with 0 mean and $Q(t)$ covariance
$w_z(k)$ the white Gaussian measurement noise matrix with 0 mean and $R(t)$ covariance
$X_g(t)$ the system states
$x_g(t)$ & $y_g(t)$ the X & Y coordinates of P_g(i.e. the current vessel position)
I_{xa} & I_{ya} the X & Y distances from P_g *to* P_a
$Z(k)$ the unit vector in Z direction
$Z_g(k)$ the measurement states

rudder and propulsion actions, vessel maneuvers can often be influenced by wind and wave excitations, where stochastic ship motions can be observed (Perera et al., 2012). Hence, such ship behavior should be incorporated into the same mathematical models to create realistic vessel navigation situations. An appropriate mathematical model that can capture the realistic behavior of ship maneuvers is considered in this study and the respective vessel states and parameters in the same are estimated in real-time to improve the accuracy of predicted ship maneuvers. One should note that the respective steering properties of the vessel can directly influence the respective state and parameter values (i.e. the mathematical model) in ship maneuvers.

The International Maritime Organization (IMO) regulations cover a significant number of required ship maneuvering capabilities, therefore vessels should be evaluated annually under various sea trials with limited environmental conditions (The Manoeuvring Committee, 2005). However, actual vessel maneuvering difficulties under varying sea conditions, i.e. various environmental effects due to wind, wave, tidal and ocean current conditions (i.e. external forces and moments), cannot be observed in these situations. Hence, ships should facilitate with sophisticated navigation aids to identify the respective vessel behavior under such environmental conditions. That can help ship navigators to make appropriate decisions under critical navigation situations. Even though modern navigation systems in air and land transportation are equipped with such facilities to improve the navigation safety (Perera and Soares, 2015), that approach has not been adopted by maritime transportation, properly. Furthermore, integrated bridge systems in ships still consist of limited navigation features and sensor configurations in some situations, where the respective technology updates have not been properly adopted. Inadequate navigation tools can compromise the safety of ship maneuvers under varying environmental conditions and question the validity of navigators' decisions in some situations. Hence, this study proposes to develop appropriate navigation tools to overcome such ship navigation challenges.

1.2. Sea trials

Several important factors that relate to ship maneuverability are identified in various sea trails. Ship turning ability is an important factor that measures the magnitudes of advance and tactical diameter of the respective vessel and that knowledge has often been used to predict possible ship behavior. These sea trials are conducted by turning a hard-over rudder to both starboard and port and measuring ship heading changes, so called “turning circle tests”. The respective hydrodynamic force and moment effects that relate to ship maneuvers under limited environmental conditions are identified in these sea trials. However, such hydrodynamic forces and moments can change due to varying environmental conditions (i.e. wind, wave, tidal and ocean currents) and those changes should be identified to improve the predictability of ship maneuvers.

The trajectory prediction features in ship maneuvers can help navigators to make better decisions in congested and confined waters, where the navigation safety should be prioritized. Furthermore, the same features may assign longer time intervals for navigators to prepare for critical ship navigation situations, such as “no point of return”, where vessels should navigate with caution after specified way points in congested and confined waters. Other critical ship navigation situations, such as crash stopping & berthing maneuvers and offshore operations, can also be benefited from the similar features. One should note that such predicted trajectories in ship maneuvers facilitate not only to make better decisions but also to re-evaluate navigation decisions, where vessel behavior can vary due to environmental variations. The same can extensively be used to evaluate various ship encounters with higher collision risk situations especially in congested and/or confined waters. Hence, ship trajectory prediction features should be a part of integrated bridge systems and that can be implemented under Electronic chart display systems (ECDISs) (Perera and Soares, 2017). Furthermore, additional ship navigation

information (i.e. ship turning ability information) can also be included in ECDISs to further improve the navigation safety.

2. Recent developments

2.1. Mathematical models

Several studies on predicting ship maneuvers are presented in the recent literature and that can be divided into two steps: state & parameter estimation and trajectory prediction. Various state & parameter estimation approaches in ship navigation are proposed by the following studies with the respective methods: linear continuous time domain model with discrete time measurements (Astrom and Kalstrom, 1976), Kalman filter (Triantafyllou et al., 1983), extended Kalman Filter and Second Order Filter (Ma and Tong, 2003), nonlinear Norrbin model (Casado et al., 2007), non-linear ship maneuvering mathematical model (Skjetne et al., 2004), Support Vector Regression (SVR) (Sheng et al., 2008), and recursive neural networks (Moreira and Soares, 2003; Rajesh and Bhattacharyya, 2008). Similarly, various trajectory prediction approaches in ship navigation are proposed by the following studies with the respective methods: neural networks (El-Tahan et al.), Maneuvering Modeling Group (MMG) standard method (Yasukawa and Yoshimura, 2015), autoregressive moving average (ARMA) and neural networks (Khan et al., 2004). However, ship navigation under constant state and parameter conditions is assumed in these studies, where the respective state and parameter adaptability for various environmental conditions is limited. Therefore, the predicted behavior may deviate from actual ship maneuvers in some situations, when vessels confront with varying wind, wave, tidal and ocean current conditions. One should note that commercial tools and techniques that are developed to predict ship maneuvers in integrated bridge systems are based on simplified mathematical models with vessel position, speed log and vessel rate of turn (ROT) measurements. Similarly, such model performance may degrade under complex ship navigation situations (i.e. varying environmental conditions) as discussed, previously.

Therefore, a novel mathematical framework that can capture such environmental variations and adapt vessel states and parameters is proposed in this study. That consists of a continuous-time curvilinear motion model with pivot point information to predict vessel positions and heading variations (i.e. heading and rate of turn (RAT)). Hence, this approach can be seen as a combination of both state & parameter estimation and trajectory prediction methods. The respective vessel states and parameters of the same model are estimated by an extended Kalman filter (EKF). Furthermore, a vector dot and cross product based algorithm is also proposed to predict a ship maneuvering trajectory for a short time interval of 30 (s), where future vessel positions and heading variations are calculated. One should note that this time interval is considered as an appropriate period for the navigator to make adequate decisions and the accuracy of a predicted vessel maneuvering trajectory is higher in such short time intervals.

2.2. Pivot point

The pivot point in a vessel can play an important role in predicting its behavior. Ship navigators often use their experience to estimate pivot point locations and predict vessel positions and orientations (i.e. heading) in the respective ship tracks (i.e. ship trajectories). Furthermore, the same term (i.e. the pivot point) has extensively been used in teaching and ship-handling training procedures as an essential technique for predicting vessel behavior.

An analytical estimate of the pivot point location can be calculated by considering linearized sway and yaw equations of a turning ship. In general, the pivot point of a ship can be defined as the center of vessel rotation consisting a zero-drift angle with respect to its velocity components (Seo and Mishu, 2011). The distance to the pivot point from the ship center of gravity can be approximated as the ratio between sway velocity and yaw rate (i.e. at the center of gravity). One should note that the pivot point in a vessel achieves the steady-state phase even under the transient phase of a turning maneuver (Tzeng, 1998), where sway velocity and yaw rate variations can still be observed. This situation occurs due to the cancellation effects among sway and yaw induced forces and moments and such information can play an important role in predicting vessel behavior. This study also proposes to use such pivot point information to predict vessel positions and orientations in a turning circle type ship maneuver within a short time interval. Furthermore, an estimation algorithm is proposed to incorporate the respective state and parameter variations due to environmental conditions.

The proposed mathematical framework consists of several steps. Firstly, an appropriate mathematical model for ship maneuvers under varying environmental conditions is derived. Secondly, the model states and parameters are estimated by an extended Kalman filter (EKF) with respect to vessel position, heading, yaw rate and acceleration measurements, where the variations in environmental conditions can be captured. Thirdly, the pivot point location with respect to the vessel center of gravity is calculated. Fourthly, the respective velocity components of the pivot point and the center of gravity of the vessel are calculated. Fifthly, the center of planar motion of the vessel is calculated by a vector dot and cross product based algorithm. Then, the distances (i.e. radiuses) from the center of planar motion to the center of gravity and pivot point of the vessel are calculated. Finally, the radiuses, i.e. the center of planar motion and the respective velocity components of the vessel, are used to predict the maneuvering trajectory for a 30 (s) interval consisting the future vessel position and orientation.

This study considers a continuous-time curvilinear motion model, a kinematic model (Perera and Soares, 2012), for ship maneuvers rather than a dynamic model (Trodden et al., 2016). To develop a dynamic model for ship maneuvers, the respective hydrodynamic force and movement effects on the vessel should be observed (i.e. measured or estimated), accurately and that can be an extremely difficult task due to unknown steering nonlinearities. However, such external force and movement effects can be incorporated into the respective acceleration components, indirectly in kinematic models of ship maneuvers. Furthermore, vessel acceleration components can be measured under several sensors (i.e. accelerometers), accurately and those measurements can be a part of the kinematic models. Hence, that is the main advantage of using a kinematic model for ship maneuvers. This study also proposes to include additional sensors for measuring vessel position, heading, yaw rate and surge and sway acceleration components and that can further improve the accuracy of predicted ship maneuvers.

3. Vessel maneuvering model

3.1. Mathematical model

The proposed mathematical model for ship maneuvers with a fixed XYZ right-hand coordinate system (i.e. North, East, Down reference frame) is presented in Fig. 1. A continuous-time curvilinear motion model that represents vessel kinematics is considered (Perera and Soares, 2012) and that can be written as (Perera et al., 2012):

$$\begin{aligned} \dot{\chi}(t) &= a_{ng}(t)/V(t) \\ \dot{V}(t) &= a_{tg}(t) \\ v_{xg}(t) &= V(t)\cos(\chi(t)) \\ v_{yg}(t) &= V(t)\sin(\chi(t)) \end{aligned} \tag{1}$$

The respective surge and sway velocity components of the vessel can be written as:

$$\begin{aligned} u(t) &= v_{xg}(t)\cos(\psi(t)) + v_{yg}(t)\sin(\psi(t)) \\ v(t) &= v_{yg}(t)\cos(\psi(t)) - v_{xg}(t)\sin(\psi(t)) \end{aligned} \tag{2}$$

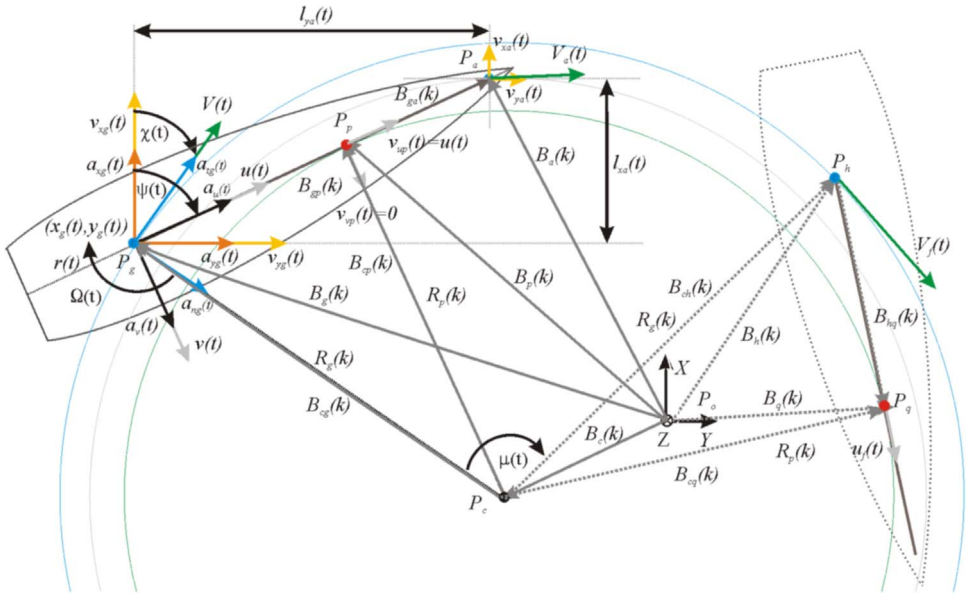

Fig. 1. Ship maneuvering model.

The time derivatives of (1) can be written as:

$$\dot{v}_{xg}(t) = a_{xg}(t) = a_{tg}(t)f^{vxg} - a_{ng}(t)f^{vyg}$$
$$\dot{v}_{yg}(t) = a_{yg}(t) = a_{tg}(t)f^{vyg} + a_{ng}(t)f^{vxg} \quad (3)$$

The respective functions in (3) can be written as:

$$f^{vyg} = \sin(\chi(t)) = v_{yg}(t)/\sqrt{v^2_{xg}(t) + v^2_{yg}(t)}$$
$$f^{vxg} = \cos(\chi(t)) = v_{xg}(t/\sqrt{v^2_{xg}(t) + v^2_{yg}(t)} \quad (4)$$

Similarly, the time derivatives of (2) can be written as:

$$\dot{u}(t) = a_u(t) = (a_{xg}(t) + r(t)v_{yg}(t))\cos\psi(t) + (a_{yg}(t) - r(t)v_{xg}(t))sin\ \psi(t)$$
$$\dot{v}(t) = a_v(t) = (a_{yg}(t) - r(t)v_{xg}(t))\cos\psi(t) - (a_{xg}(t) + r(t)v_{yg}(t))sin\ \psi(t) \quad (5)$$

3.2. System model

As the next step of this study, the ship maneuvering model in (1) is summarized and that can be written as:

$$\dot{X}_g(t) = f(X_g(t)) + w_g(t)$$
$$E[w_g(t)] = 0$$
$$E[w_g(t), w_g(t)] = [Q\ \ (t)] \quad (6)$$

The respective vessel states and function in (6) can be written as:

$$X_g(t) = [x_{xg}(t)\quad v_{xg}(t)\quad y_{xg}(t)\quad v_{yg}(t)\quad u(t)\quad v(t)\quad \psi(t)\quad r(t)\quad a_{tg}(t)\quad a_{ng}(t)]^T$$
$$f(X_g(t)) = [v_{xg}(t)\quad a_{xg}(t)\quad v_{yg}(t)\quad a_{yg}(t)\quad a_u(t)\quad a_v(t)\quad r(t)\quad 0\quad 0\quad 0]^T \quad (7)$$

3.3. Measurement model

As the next step, the respective vessel states and parameters in (6) should be estimated. That can be done by selecting a set of measurable vessel states and parameters and categorized as a measurement model. A discrete-time measurement model is considered due to the availability of sensor values in discrete time instants. It is assumed that vessel position (by GPS/GDPS systems), heading and yaw rate (by heading and yaw-rate sensors) and surge and sway acceleration (by accelerometers) components are measured by the respective sensors. Hence, the measurement model can be written as:

$$Z_g(k) = h(X_g(k)) + w_z(k),\quad k = 1, 2, \ldots$$
$$E[w_z(k)] = 0$$
$$E[w_z(k), w_z(k)] = [R(k)] \quad (8)$$

The respective function in (8) can be written as:

$$h(X_g(k)) = [x_g(k)\quad y_g(k)\quad \psi(k)\quad r(k)\quad a_u(k)\quad a_v(k)]^T \quad (9)$$

A negligible correlation between system and measurement noise is assumed and denoted as $E[w_g(t), w_z(k)] = 0$ for all k and t.

3.4. Estimation algorithm

Various EKF and KF based applications are implemented for transportation systems in the recent literature (Brown and Hwang, 1997; Tiano et al., 2007; Perera et al., 2016; Del Gobbo et al., 2001). An EKF algorithm is proposed in this study also to estimate the required vessel states and parameters, as mentioned previously. An overview of an EKF algorithm and its implementation steps for a vessel state and parameter estimation situation are presented in Perera et al. (2012). Similar steps are implemented with the EKF algorithm in study to estimate the respective vessel states and parameter by considering (6) and (8).

4. Maneuvering prediction

4.1. Vector calculations

The vessel states and parameters, estimated by an EKF algorithm, are considered in this section to derive the respective navigation vectors. One should note that these vectors represent current navigation conditions (i.e. current vessel position, heading, velocity, and acceleration components) of the vessel. However, these same vectors can be used to estimate future navigation conditions (i.e. future vessel position, heading, velocity, and acceleration components) of the vessel by assuming constant navigation conditions with a short time interval. Even though constant vessel state and parameter conditions are

assumed in this approach, the model in (6) can adopt the respective variations because of the EKF algorithm. Therefore, (6) can be used to approximate complicated ship maneuvers under varying environmental conditions.

The estimated vessel states and parameters are used to calculate the coordinates of the center of planar motion and pivot point of the vessel in the next step. Assuming the vessel as a rigid body, the relationship between velocity vectors of two points in terms of its angular velocity (i.e. yaw rate) is considered in this step (Ginsberg, 2008). Hence, the velocity vector at P_a can be written as:

$$V_a(k) = V\ \ (k) + \Omega(k) \times B_{ga}(k) \tag{10}$$

The respective course-speed and velocity vectors at P_g and P_a can also be written as:

$$\begin{aligned} V(k) &= \begin{bmatrix} v_{xg}(k) & v_{yg}(k) & 0 \end{bmatrix} \\ V_a(k) &= \begin{bmatrix} v_{xa}(k) & v_{ya}(k) & 0 \end{bmatrix} \end{aligned} \tag{11}$$

The yaw rate vector of the vessel can be written as:

$$\Omega(k) = \begin{bmatrix} 0 & 0 & r(k) \end{bmatrix} \tag{12}$$

The relative distance vector from P_g to a general point located along the ship centerline (i.e. P_a) can be written as:

$$B_{ga}(k) = \begin{bmatrix} l_{xa}(k) & l_{ya}(k) & 0 \end{bmatrix} \tag{13}$$

Considering (11), (12) and (13), (10) can be resulted in:

$$V_a(k) = \begin{bmatrix} v_{xg}(k) - r(k)l_{ya}(k) & v_{yg}(k) + r(k)l_{xa}(k) & 0 \end{bmatrix} \tag{14}$$

Considering (11) and (14), the respective velocity components can be written as:

$$\begin{aligned} v_{xa}(k) &= v_{xg}(k) - r(k)l_{ya}(k) \\ v_{ya}(k) &= v_{yg}(k) + r(k)l_{xa}(k) \end{aligned} \tag{15}$$

Assuming that P_a coincides with the pivot point of the vessel (i.e. $P_p \equiv P_a$), the velocity components at the pivot point can be derived as:

$$\begin{aligned} v_{xp}(k) &= v_{xg}(k) - r(k)l_{yp}(k) \\ v_{yp}(k) &= v_{yg}(k) + r(k)l_{xp}(k) \end{aligned} \tag{16}$$

The surge and sway velocity components of the pivot point by considering $v_{xp}(t)$ and $v_{yp}(t)$ can also be written as:

$$\begin{aligned} v_{up}(k) &= v_{xp}(k)\cos(\psi(k)) + v_{yp}(k)\sin(\psi(k)) = u(k) \\ v_{vp}(k) &= -v_{xp}(k)\sin(\psi(k)) + v_{yp}(k)\cos(\psi(k)) = 0 \end{aligned} \tag{17}$$

Applying (16) into (17), that resulted in:

$$\begin{aligned} &v_{xg}(k)\cos(\psi(k)) + v_{yg}(k)\sin(\psi(k)) = u(k) + r(k)l_{yp}(k)\cos(\psi(k)) - r(k)l_{xp}(k) \\ &\sin(\psi(k))v_{xg}(t)\sin(\psi(t)) - v_{yg}(t)\cos(\psi(t)) = r(t)(l_{yp}(t)sin(\psi(t)) + l_{xp}(t)cos(\psi(t))) \end{aligned} \tag{18}$$

Furthermore, (18) can be also be simplified as:

$$\begin{aligned} l_{yp}(k)\cos(\psi(k)) &= l_{xp}(k)\sin(\psi(k)) \\ v(k) &= -\ r(k)(l_{yp}(k)\sin(\psi(k)) + l_{xp}(k)\cos(\psi(k))) \end{aligned} \tag{19}$$

The magnitude of $B_{gp}(k)$ can be written as:

$$\|B_{gp}(k)\|_2 = l_{yp}(k)\sin(\psi(k)) + l_{xp}(k)\cos(\psi(k)) \tag{20}$$

Applying (19) into (20), that resulted in:

$$-v(k) = r(k)\|B_{gp}(k)\|_2 \tag{21}$$

One should note that (21) denotes the popular expression for the pivot point location with respect to the center of gravity and sway and yaw velocity components of vessels. Considering (19), the X and Y distances from the center of gravity to the pivot point can be written as:

$$\begin{aligned} l_{xp}(k) &= -\frac{v(k)}{r(k)}\cos(\psi(k)) \\ l_{yp}(k) &= -\frac{v(k)}{r(k)}\sin(\psi(k)) \end{aligned} \tag{22}$$

4.2. Trajectory prediction

An appropriate vector dot and cross product based algorithm is derived in this section to calculate the radiuses of the center of gravity and pivot point with respect to the center of planar motion of the vessel. One should note that the predicted trajectory in ship maneuvering is derived by considering these radiuses. $B_{cp}(k)$ can be written as a cross product between two vectors (Ginsberg, 2008):

$$B_{cp}(k) = \alpha(k)B_{gp}(k) \times Z(k) = \begin{bmatrix} \alpha(k)l_{yp}(k) & -\alpha(k)l_{xp}(k) & 0 \end{bmatrix} \tag{23}$$

Similarly, $B_{cg}(k)$ can be written as a cross product between two vectors as:

$$B_{cg}(k) = \beta(k)V\ \ (k) \times Z(k) = \begin{bmatrix} \beta(k)v_{yg}(k) & -\beta(k)v_{xg}(k) & 0 \end{bmatrix} \tag{24}$$

$B_{gp}(k)$ can be written as:

$$B_{gp}(k) = \begin{bmatrix} l_{xp}(k) & l_{yp}(k) & 0 \end{bmatrix} \tag{25}$$

Furthermore, $B_{gp}(k)$ can also be written as:

$$B_{gp}(k) = -\ B_{cg}(k) + B_{cp}(k) \tag{26}$$

Applying (23) and (24) into (26), the respective vector components in (25) and (26) can be compared as:

$$\begin{aligned} l_{xp}(k) &= \alpha(k)l_{yp}(k) - \beta(k)v_{yg}(k) \\ l_{yp}(k) &= \beta(k)v_{xg}(k) - \alpha(k)l_{xp}(k) \end{aligned} \tag{27}$$

Considering (27), the respective scale factors can be written as:

$$\begin{aligned} \alpha(k) &= \frac{v_{xg}(k)l_{xp}(k) + v_{yg}(k)l_{yp}(k)}{l_{yp}(k)v_{xg}(k) - l_{xp}(k)v_{yg}(k)} \\ \beta(k) &= \frac{l_{xp}{}^2(k) + l_{yp}{}^2(k)}{l_{yp}(k)v_{xg}(k) - l_{xp}(k)v_{yg}(k)} \end{aligned} \tag{28}$$

$B_g(k)$ can be written as:

$$B_g(k) = \begin{bmatrix} x_g(k) & y_g(k) & 0 \end{bmatrix} \tag{29}$$

Considering (24) and (29), $B_c(k)$ can be written as:

$$B_c(k) = B_g(k) - B_{cg}(k) = [\,x_g(k) - \beta(k)v_{yg}(k) \quad y_g(k) + \beta(k)v_{xg}(k) \quad 0\,] \tag{30}$$

Considering (22) and (23), the radius of the pivot point with respect to the center of planar motion of the vessel can be written as:

$$\|B_{cp}(k)\|_2 = R_p(k) = \alpha(k)\sqrt{l_{xp}^2(k) + l_{yp}^2(k)} = \alpha(k)\frac{v(k)}{r(k)} \tag{31}$$

Considering (24), the radius of the center of gravity with respect to the center of planar motion of the vessel can be written as:

$$\|B_{cg}(k)\|_2 = R_g(k) = \beta(k)\sqrt{v_{xg}^2(k) + v_{yg}^2(k)} \tag{32}$$

One should note that (30)–(32) are used for predicting ship maneuvers, where the future vessel position and orientation conditions are estimated. That is done by considering the respective vectors of $B_{ch}(k)$ and $B_{cq}(k)$ (see Fig. 1). Hence, $B_h(k)$ can be written as:

$$B_h(k) = \begin{bmatrix} x_h(k) & y_h(k) & 0 \end{bmatrix} \tag{33}$$

Similarly, $B_q(k)$ can be written as:

$$B_q(k) = \begin{bmatrix} x_q(k) & y_q(k) & 0 \end{bmatrix} \tag{34}$$

Considering (30) and (33), $B_{ch}(k)$ can be written as:

$$B_{ch}(k) = B_h(k) - B_c(k) = \left[x_h(k) - x_g(k) + \beta(k)v_{yg}(k)y_h(k) - y_g(k) - \beta(k)v_{xg}(k)0\right] \tag{35}$$

Considering (30) and (34), $B_{cq}(k)$ can be written as:

$$B_{cq}(k) = B_q(k) - B_c(k) = \left[x_q(k) - x_g(k) + \beta(k)v_{yg}(k)y_q(k) - y_g(k) - \beta(k)v_{xg}(k)0\right] \tag{36}$$

The respective parameters of (35) and (36) are derived in the following section. Assuming constant vessel state and parameter conditions within a short time interval, δt, the vessel rotational angle (i.e. the angle between the present and future vessel positions) around the center of planar motion can be written as (see Fig. 1):

$$\mu(k) = \frac{V(k)\delta t}{\|B_{cg}(k)\|_2} \tag{37}$$

Hence, (37) is used to derive the X and Y coordinates of the center of gravity and pivot point of the future vessel position as presented in the following calculations. A dot product between two vectors in (24) and (35) can be written as (Ginsberg, 2008):

$$B_{cg}(k)\cdot B_{ch}(k) = \|B_{cg}(k)\|_2^2 \cos\mu(k) \tag{38}$$

where $\|B_{cg}(k)\|_2 = \|B_{ch}(k)\|_2$. Hence, (38) can be written as:

$$v_{yg}(k)x_h(k) - v_{xg}(k)y_h(k) = \beta(k)\left(v_{xg}^2(k) + v_{yg}^2(k)\right)(cos\,\mu(k) - 1) + x_g(k)v_{yg}(k) - y_g(k)v_{xg}(k) \tag{39}$$

Similarly, a cross product between two vectors in (24) and (35) can be written as (Ginsberg, 2008):

$$B_{cg}(k) \times B_{ch}(k) = \left[0 \quad 0 \quad \|B_{cg}(k)\|_2^2 \sin\mu(k)\right] \tag{40}$$

Hence, the respective vector components in (40) can be derived as:

$$v_{xg}(k)x_h(k) + v_{yg}(k)y_h(k) = \beta(k)\left(v_{xg}{}^2(k) + v_{yg}{}^2(k)\right)sin\,\mu(k) + v_{yg}(k)y_g(k) + v_{xg}(k)x_g(k) \tag{41}$$

Considering (39) and (41), the following results can be derived:

$$\begin{aligned} x_h(k) &= x_g(k) + \beta(k)(v_{xg}(k)\sin\mu(k) + v_{yg}(k)(\cos\mu(k) - 1)) \\ y_h(k) &= y_g(k) + \beta(k)(v_{yg}(k)\sin\mu(k) + v_{xg}(k)(\cos\mu(k) - 1)) \end{aligned} \tag{42}$$

One should note that (42) represents the X and Y coordinates of the center of gravity of the future vessel position. Similarly, a dot product between two vectors in (23) and (36) can be written as:

$$B_{cp}(k)\cdot B_{cq}(k) = \|B_{cp}(k)\|_2^2 \cos\mu(k) \tag{43}$$

where $\|B_{cp}(k)\|_2 = \|B_{cq}(k)\|_2$. Hence, (43) can be derived as:

$$l_{yp}(k)x_q(k) - l_{xp}(k)y_q(k) = \alpha(k)(l_{xp}^2(k) + l_{yp}^2(k))cos\,\mu(k) + l_{yp}(k)x_g(k) - l_{yp}(k)\beta(k)v_{yg}(k) - l_{xp}(k)y_g(k) - l_{xp}(k)\beta(k)v_{xg}(k) \tag{44}$$

Similarly, a cross product between two vectors in (23) and (36) can be written as:

$$B_{cp}(k) \times B_{cq}(k) = \left[0 \quad 0 \quad \|B_{cp}(k)\|_2^2 \sin\mu(k)\right] \tag{45}$$

Hence, the respective vector components in (45) can be derived as:

$$x_q(k)l_{xp}(k) + y_q(k)l_{yp}(k) = \alpha(k)\left(l_{xp}^2(k) + l_{yp}^2(k)\right)sin\,\mu(k) + x_g(k)l_{xp}(k) - \beta(k)l_{xp}(k)v_{yg}(k) + y_g(k)l_{yp}(k) + \beta(k)l_{yp}(k)v_{xg}(k) \tag{46}$$

Considering (44) and (46), the following result can be derived:

$$\begin{aligned} x_q(k) &= x_g(k) + \alpha(k)\left(l_{yp}(k)cos\,\mu(k) + l_{xp}(k)sin\,\mu(k)\right) - \beta(k)v_{yg}(k)y_q(k) \\ &= y_g(k) + \alpha(k)\left(l_{yp}(k)sin\,\mu(k) - l_{xp}(k)cos\,\mu(k)\right) + \beta(k)v_{xg}(k) \end{aligned} \tag{47}$$

One should note that (47) represents the X and Y coordinates of the pivot point of the future vessel position. Hence, $B_{hq}(k)$ can be written as:

$$B_{hq}(k) = B_q(k) - B_h(k) = \left[x_q(k) - x_h(k) \quad y_q(k) - y_h(k) \quad 0\right] \tag{48}$$

However, (48) can be simplified and presented in the following calculations, where the unit scaled heading vector for the future vessel position is derived. A dot product between $B_{hq}(k)$ and the unit vector of X direction can be written as:

$$B_{hq}(k)\cdot X = \|B_{hq}(k)\|_2 \cos\psi_f(k) \tag{49}$$

Considering (49), the cosine value of the heading of the future vessel position can be written as:

$$\cos\psi_f(k) = \mathrm{sgn}(\cos\psi(k))\left\|\frac{x_q(k) - x_h(k)}{\sqrt{(x_q(k) - x_h(k))^2 + \left(y_q(k) - y_h(k)\right)^2}}\right\|_2 \tag{50}$$

Similarly, a cross product between $B_{hq}(k)$ and the unit vector of X direction can be written as:

$$B_{hq}(k) \times X = \left[0 \quad 0 \quad \|B_{hq}(k)\|_2 \sin\psi_f(k)\right] \tag{51}$$

Considering (51), the sine value of the heading of the future vessel position can be written as:

$$\sin\psi_f(k) = \mathrm{sgn}(\sin\psi(k))\left\|\frac{y_q(k) - y_h(k)}{\sqrt{(x_q(k) - x_h(k))^2 + \left(y_q(k) - y_h(k)\right)^2}}\right\|_2 \tag{52}$$

One should note that (50) and (52) are incorporated with the current vessel heading information to improve the prediction accuracy of the vessel heading. Hence, the unit scaled heading vector for the future vessel position can be written as:

$$\overline{B}_{hq}(k) = \left[\cos\psi_f(k) \quad \sin\psi_f(k) \quad 0\right] \tag{53}$$

5. Computational simulations

The respective computational simulations under the proposed mathematical framework to predict ship maneuvers are presented in this section. The actual vessel states and parameters are simulated and the measurements are created by adding the respective sensor noise into the actual vessel state and parameter values. The estimated vessel states and parameters are calculated by the EKF algorithm. The actual (Act. Traj.) and estimated (Est. Traj.) navigation trajectories for a ship maneuvering situation are presented in Fig. 2. The actual navigation trajectory is simulated in this study and the EKF algorithm is used to calculate the estimated trajectory (Perera and Soares, 2012), as mentioned before. To improve the visibility of the figure, the estimated trajectory positions in selected time intervals are presented. Furthermore, the scaled heading vectors for each vessel position are also presented in the same figure. A predicted trajectory segment for the same vessel maneuver is presented in Fig. 3 and a zoomed view of the same situation is presented in Fig. 4 with the actual and estimated vessel trajectories.

As presented in the figures, the actual vessel positions are denoted by blue vessel icons with dotted lines and the current vessel position is presented in a black vessel icon with continues lines. The future vessel position and predicted trajectory are presented in cyan vessel icons with continues lines. The pivot point movements within a selected time interval are presented in magenta stars (see Fig. 3). Furthermore, the pivot point relationships to the vessel center of gravity are also presented as continuous blue lines. One should note that (30)–(32)

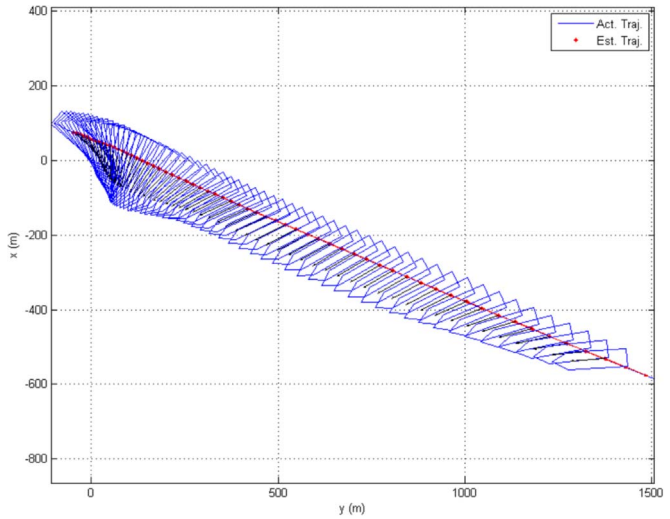

Fig. 2. The respective vessel positions and orientations along the vessel trajectory: Situation 1. (For interpretation of the references to color in this figure, the reader is referred to the web version of this article).

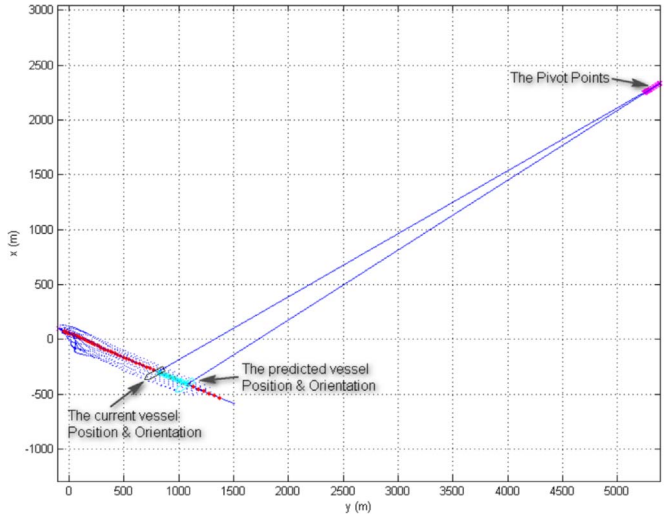

Fig. 3. The current and predicted vessel positions and orientations along the vessel trajectory: Situation 1. (For interpretation of the references to color in this figure, the reader is referred to the web version of this article).

are used to create the predicted trajectory (i.e. the future vessel position) that consists of the center of planar motion, radiuses of the pivot point and center of gravity with respect to the center of planar motion of the vessel. Similarly, (42), (47) and (53) are used to calculate the X and Y coordinates of the center of gravity, pivot point and heading of the future vessel position. The results show that the proposed mathematical framework can be used to predict ship maneuvers, i.e. the future vessel position and orientation, successfully.

Furthermore, the respective vessel velocity components, $v_{xg}(t)$ and $v_{yg}(t)$, of actual (Act.) and estimated (Est.) values for the same ship maneuver are presented in the top plot of Fig. 5. The measured vessel positions are used by the EKF algorithm, therefore the estimated values of vessel velocity components converge quickly to the actual values in this plot. The respective vessel acceleration components, $a_{ng}(t)$ and $a_{tg}(t)$, of actual (Act.) and estimated (Est.) values for the same ship maneuver are presented in the bottom plot of Fig. 5. The measured surge & sway acceleration components are used by the EKF algorithm, therefore the estimated values of vessel normal and tangential acceleration components converge slowly to the actual values in this plot (i.e. due to the model complexity).

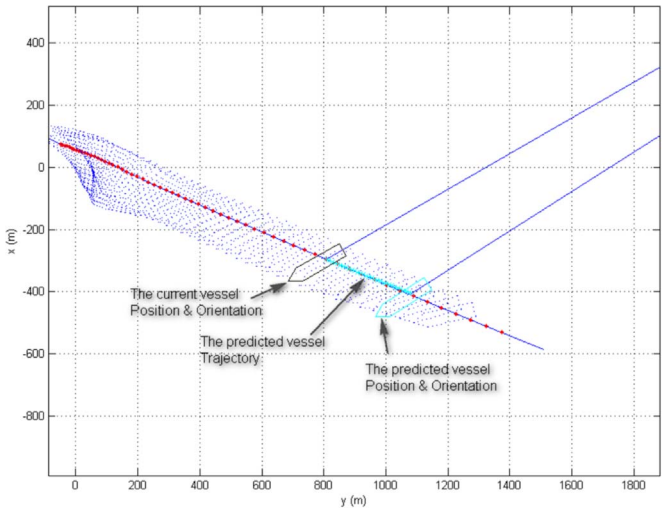

Fig. 4. The current and predicted vessel positions and orientations along the vessel trajectory (zoomed view): Situation 1. (For interpretation of the references to color in this figure, the reader is referred to the web version of this article).

At the initial execution step of the EKF algorithm, guess state and parameter values (i.e. some selected reasonable values) are introduced into the algorithm. Therefore, some errors between the actual and estimated vessel states and parameters can be noted in the same plots and this situation occurs only in the initial execution step of the EKF algorithm. However, the EKF algorithm eventual reduces the state and parameter errors during its execution process, therefore the estimated values of vessel states and parameters converge to the actual values, appropriately. One should note that the EKF algorithm traces the actual vessel states and parameters, continuously (i.e. without any time delay with the required state and parameter accuracy) during its execution process. Furthermore, an adequate mathematical model in ship maneuvering should be incorporated with the EKF algorithm to estimate the unmeasured vessel (i.e. unobservable) states and parameters, successfully. In general, the measured (i.e. observable) vessel states and parameters are estimated faster, and the unmeasured (i.e. unobservable) states and parameters are estimated slower in such situations.

The respective vessel headings, $\psi(t)$, of actual (Act.), measured (Mea.) and estimated (Est.) values for the same ship maneuver are presented in the top plot of Fig. 6. Similarly, the respective vessel yaw rates, $r(t)$, of actual (Act.), measured (Mea.) and estimated (Est.) values are presented in the bottom plot of Fig. 6. The measured heading and yaw rate values are used by the EKF algorithm, therefore the estimated values of the same converge quickly to the actual values in this figure. The respective vessel surge and sway velocity components, $u(t)$ and $v(t)$, of actual (Act.) and estimated (Est.) values for the same ship maneuver are presented in Fig. 7. The measured vessel positions and accelerations are used by the EKF algorithm, therefore the estimated values of the same velocity components converge slowly to the actual values in this plot (i.e. due to the model complexity).

The EKF algorithm estimates (i.e. a continuous-time curvilinear motion model with pivot point information) the respective vessel states and parameters and the vector product based algorithm predicts the future vessel position and orientation, adequately under the simulated data. That are categorized as the success in the proposed mathematical framework in predicting ship maneuvers. It is also noted that the pivot point can achieve a steady state even under sway speed and yaw rate variations (i.e. the vessel is still in the transient phase) in a turning circle type maneuver and that concept also improves the accuracy of the predicted vessel maneuver. One should note that this study assumes that the center of planar motion of the vessel is fixed during the prediction period. However, it is also noted that the center of planar

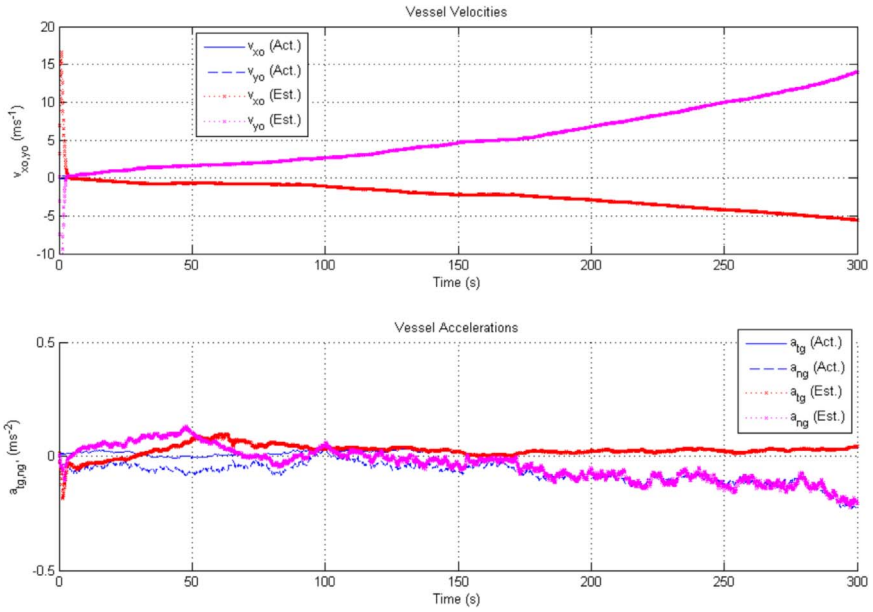

Fig. 5. Vessel velocity and acceleration components: Situation 1.

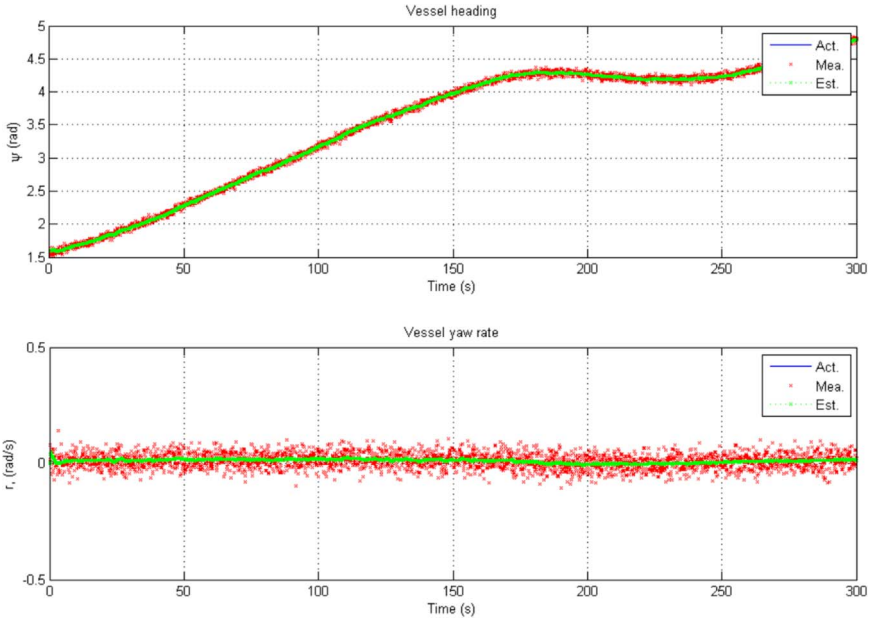

Fig. 6. Vessel heading and yaw rate components: Situation 1.

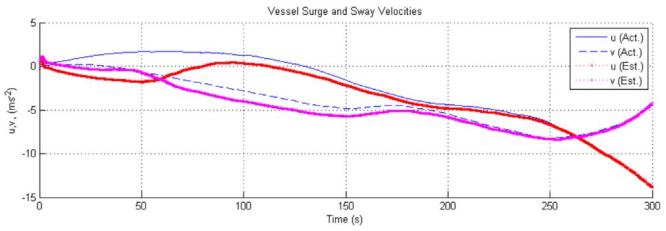

Fig. 7. Vessel surge and sway velocity components: Situation 1.

motion may change significantly due to external environmental conditions. Therefore, this behavior (i.e. the variations on the vessel center of planar motion) should also be incorporated into this mathematical framework to improve the accuracy, further. That can be done by estimating the future behavior of the center of planar motion by considering the past and present vessel motions and that feature is considered as the future work of this study. Furthermore, additional vessel maneuvers with the actual and predicted vessel position and heading conditions under the EKF algorithm are presented in Figs. 8–11.

6. Conclusion

Ship maneuvers are predicted by using kinematic models, dynamic models or combined models (both kinematics and dynamics), as discussed previously. However, the implementation of dynamic models in ship maneuvers can be a complex process due the respective nonlinear hydrodynamic forces and moments, where the respective vessel states and parameters for such models cannot often be measured (i.e. observed), directly. Furthermore, the system-model uncertainties

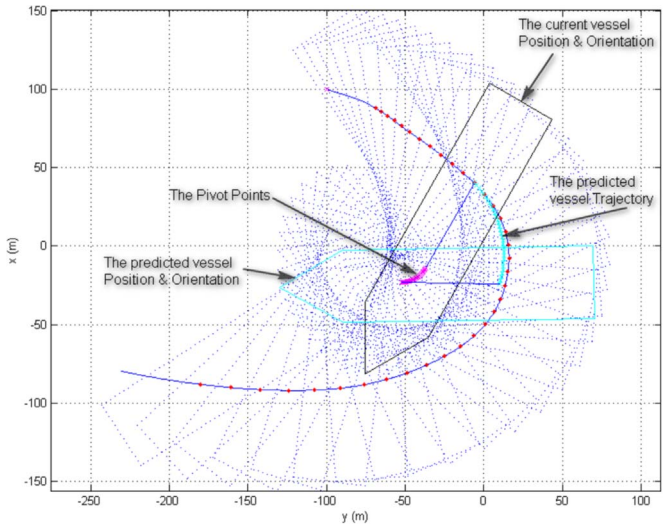

Fig. 8. The current and predicted vessel positions and orientations along the vessel: Situation 2.

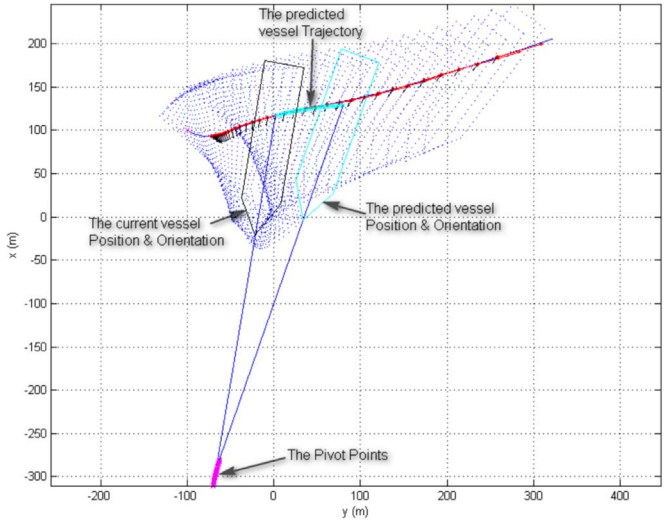

Fig. 9. The current and predicted vessel positions and orientations along the vessel: Situation 3.

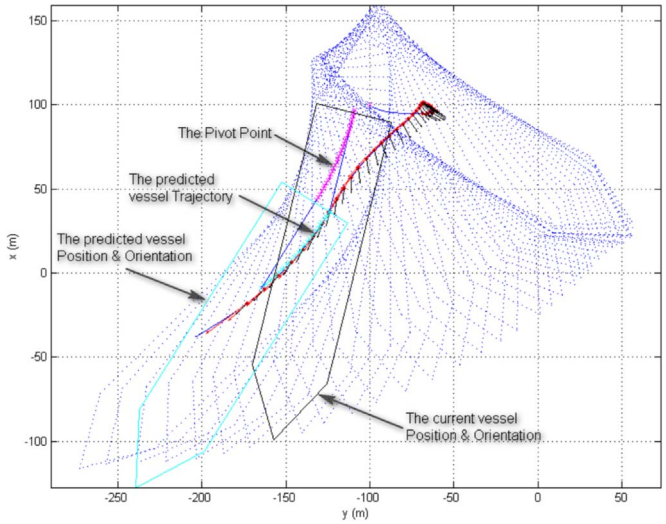

Fig. 10. The current and predicted vessel positions and orientations along the vessel: Situation 4.

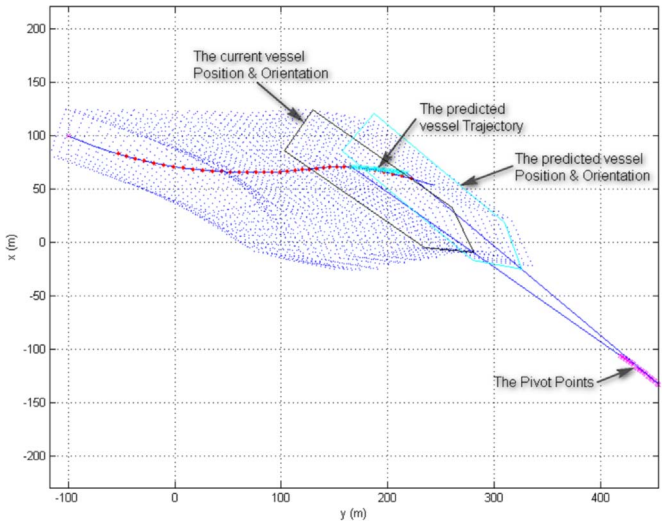

Fig. 11. The current and predicted vessel positions and orientations along the vessel: Situation 5.

in such dynamic models can further diverge parameter estimation algorithms and that eventual degrade the accuracy of predicted ship maneuvers. Therefore, a novel kinematic-based mathematical framework for predicting ship maneuvers for a short time interval is proposed in this study and that overcomes the respective challenges that are associated with dynamic models.

Even though various kinematic models are considered under other research studies (i.e. especially in robotics) (Klančar and Škrjanc, 2007; Fukao et al., 2000; Jones and Walker, 2006; Zhuang et al., 1992), the same concept can be a novel approach to maritime transportation, where several dynamic models and combined models (both kinematics and dynamics) have been implemented. The main advantage in such kinematic models is that the modeling difficulties of complex vessel dynamic conditions can be avoided. However, the respective vessel dynamics are included within acceleration components and such accelerations should be measured accurately to succeed with kinematic models. Therefore, a considerable number for system states and parameters should be measured under kinematic models to support state and parameter estimation algorithms.

If the vessel has constant state and parameter values in a maneuvering situation, then that will rotate in a perfect circle. The EKF algorithm is not required in such situations and the respective radius information can be used to predict the future vessel position and orientation of the ship maneuver. In general, vessel states and parameters slightly vary within the same ship maneuver due to environmental conditions and that can be captured by the EKF algorithm. One should note that vessel responses can be somewhat slow, even though environmental conditions can change, quickly. The proposed kinematic-based mathematical framework that often derives smooth parabolic type of trajectories in a short time interval is well suited for such situations (i.e. slow varying vessel motions) as presented in the respective computational results. However, there are several challenges can also be observed under the same framework. One should note that the continuous-time curvilinear motion model for ship maneuvers can be developed under various combinations of vessel states and parameters. It is difficult to observe the respective vessel state and parameter interactions in such nonlinear models, therefore the optimal state and parameter combination (i.e. the perfect ship maneuvering model and measurement model for the EKF algorithm) cannot be identified under the present techniques. Hence, several curvilinear motion models (i.e. various state and parameter combinations) to predict ship maneuvers are developed and the model with the most promising simulation results is presented in this study. It is believed that the success in such curvilinear motion model relates to

the EKF algorithm and its interactions with various combinations of vessel states and parameters.

Furthermore, slight deviations of actual and predicted vessel positions and orientations are observed in the computational simulations and such situations can also be expected in realistic sea going situations. One should note that future environmental conditions that may introduce unexpected external forces and moments in ship maneuvers cannot always be predicted, accurately. Such effects can also influence vessel velocity and acceleration components and introduce slight deviations in actual and predicted vessel positions and orientations. Furthermore, various erroneous conditions (i.e. sensor faults and time delays) in the respective systems and sensors can introduce additional uncertainties in predicted vessel positions and orientations.

Therefore, additional steps should be taken to quantify the respective uncertainties in actual and predicted vessel positions and orientations. A possible navigation range, where the vessel can be located within a selected time interval can be included in such situations to quantify such maneuvering uncertainties. Furthermore, vessel turning rate information for starboard and port can also be used to create such possible navigation range. The information on ship turning ability (i.e. the magnitudes of advance and tactical diameter) that relates to vessel respective acceleration components (i.e. mean and variance values) can also be used to support the same. The respective acceleration components have also been used by the proposed mathematical framework to predict the respective ship maneuvers. Hence, these additional steps can further improve the propose framework as the future work of this study. That can be implemented in ship integrated bridge systems to estimate vessel states and parameters and estimate future vessel positions and orientations. The predicted position and orientation information can be used for assessing of prior collision situations among vessels and that improve the safety of ship navigation as a decision support tool.

References

Astrom, K.J., Kalstrom, C.G., 1976. Identification of ship steering dynamics. Automatica 12, 9–12.

Brown, G.G., Lawphongpanich, S., Thurman, K.P., 1994. Optimizing ship berthing. Nav. Res. Logist. 41 (1), 115.

Brown, R.G., Hwang, P.Y.C., 1997. Introduction to Random Signals and Applied Kalman Filtering. John Wiely & Sons, New York, USA.

Casado, M.H., Ferreiro, R., Velasco, F.J., 2007. Identification of nonlinear ship model parameters based on the turning circle test. J. Ship Res. 51 (2), 174–181.

Del Gobbo, D., Napolitano, M., Famouri, P., Innocenti, M., 2001. Experimental application of extended Kalman filtering for sensor validation. IEEE Trans. Control Syst. Technol. 9 (2), 376–380.

Divelbiss, A.W., Wen, J.T., 1997. Trajectory tracking control of a car-trailer system. IEEE Trans. Control Syst. Technol. 5 (3), 269–278.

El-Tahan, M., El-tahan, H., Tuer, K., Rossi, M., Advanced Ship Autopilot System. Patent US 6 611 737 B1.

Fukao, T., Nakagawa, H., Adachi, N., 2000. Adaptive tracking control of a nonholonomic mobile robot. IEEE Trans. Robot. Autom. 16 (5), 609–615.

Ginsberg, J., 2008. Engineering Dynamics. Cambridge University Press, Cambridge, UK, 173–175.

Jones, B.A., Walker, I.D., 2006. Kinematics for multisection continuum robots. IEEE Trans. Robot. 22 (1), 43–55.

Khan, A., Bil, C., Marion, K., Crozier, M., 2004. Real time prediction of ship motions and attitude using advanced prediction techniques. In: Proceedings of the 24th International conference of the Aeronautical Sciences.

Klančar, G., Škrjanc, I., 2007. Tracking-error model-based predictive control for mobile robots in real time. Robot. Auton. Syst. 55 (6), 460–469.

Ma, F.C., Tong, S.H., 2003. Real-time parameters identification of ship dynamic using the extended Kalman filter and the second order filter. In: Proceedings of 2003 IEEE Conference on Control Applications (CCA 2003). Vol. 2, June 2003, pp. 1245–1250.

Ministry of Infrastructures and Transports. Marine Casualties Investigative Body, Italy, “Cruise Ship Costa Concordia Marine Casualty on January 13, 2012”. Report on the safety technical investigation.

Moreira, L., Soares, C. Guedes, 2003. Dynamic model of maneuverability using recursive neural networks. Ocean Eng. 30 (13), 1669–1697.

Paley, D., Zhang, F., Leonard, N.E., 2008. Cooperative control for ocean sampling: the glider coordinated control system. IEEE Trans. Control Syst. Technol. 16 (4), 735–744.

Pathirana, P.N., Savkin, A.V., Sanjay, Jha, 2004. Location estimation and trajectory prediction for cellular networks with mobile base stations. IEEE Trans. Veh. Technol. 53 (6), 1903–1913.

Perera, L.P., Soares, C. Guedes, 2012. Sliding mode controls in partial feedback linearization applied unstable ship steering. In: Proceedings of the 9th IFAC Conference on Manoeuvring and Control of Marine Craft (MCMC 2012). Arenzano, Italy, September 2012.

Perera, L.P., Soares, C.Guedes, 2012. Vector-product based collision estimation and detection in e-navigation. In: Proceedings of the 9th IFAC Conference on Manoeuvring and Control of Marine Craft (MCMC 2012). Arenzano, Italy, September 2012,pp. 164–169.

Perera, L.P., Soares, C. Guedes, 2015. Collision risk detection and quantification in ship navigation with integrated bridge systems. J. Ocean Eng. 109, 344–354.

Perera, L.P., Soares, C. Guedes, 2017. Weather routing and safe ship handling in the future of shipping. J. Ocean Eng. 130, 684–695.

Perera, L.P., Oliveira, P., Guedes Soares, C., 2012. Vessel detection, tracking, state estimation and navigation trajectory prediction for the vessel traffic monitoring and information process. IEEE Trans. Intell. Transp. Syst. 13 (3), 1188–1200.

Perera, L.P., Carvalho, J.P., Guedes Soares, C., 2014a. Solutions to the failures and limitations of mamdani fuzzy inference in ship navigation. IEEE Trans. Veh. Technol. 63 (4), 1539–1554.

Perera, L.P., Ferrari, V., Santos, F.P., Hinostroza, M.A., Soares, C. Guedes, 2014b. Experimental evaluations on ship autonomous navigation & collision avoidance by intelligent guidance. IEEE J. Ocean. Eng.. http://dx.doi.org/10.1109/JOE.2014.2304793.

Perera, L.P., Oliveira, P., Soares, C. Guedes, 2016. System identification of vessel steering with unstructured uncertainties by persistent excitation maneuvers. IEEE J. Ocean. Eng. 41 (3), 515–528.

Rajesh, G., Bhattacharyya, S.K., 2008. System identification for nonlinear maneuvering of large tankers using artificial neural network. Appl. Ocean Res. 30, 256–263.

Seo, S.G., Mishu, M., 2011. The use of pivot point in ship handling for safer and more accurate ship manoeuvring. In: Proceedings of IMLA. Opatija, Croatia, October 2011,pp. 271–280.

Sheng, L., Jia, S., Bing, L., Gao-yun, L., 2008. Identification of ship steering dynamics based on aca-svr. In: Proceeding of 2008 IEEE International Conference on Mechatronics and Automation, pp. 514–519.

Skjetne, R., Smogeli, O.N., Fossen, T.I., 2004. A nonlinear ship maneuvering model: identification and adaptive control with experiments for a model ship. Model. Identif. Control 25 (1), 3–27.

The Manoeuvring Committee, 2005. Final report and recommendations to the 24th ITTC. In: Proceedings of the 24th ITTC. UK, vol I, pp. 137–198.

Tiano, A., Sutton, R., Lozowicki, A., Naeem, W., 2007. Observer Kalman filter identification of an autonomous underwater vehicle. Control Eng. Pract. 15 (6), 727–739.

Triantafyllou, M.S., Bodson, M., Athans, M., 1983. Real time estimation of ship motions using Kalman filtering techniques. IEEE J. Ocean. Eng. 8 (1), 9–20.

Trodden, D.G., Woodward, M.D., Atlar, M., 2016. Accounting for ship manoeuvring motion during propeller selection to reduce CO_2 emissions. Ocean Eng. 123 (1), 346–356.

Tzeng, C.Y., 1998. Analysis of the pivot point for a turning ship. J. Mar. Sci. Technol. 6 (1), 39–44.

Yasukawa, H., Yoshimura, Y., 2015. Introduction of MMG standard method for ship maneuvering predictions. J. Mar. Sci. Technol. 20 (1), 37–52.

Zhuang, H., Roth, Z.S., Hamano, F., 1992. A complete and parametrically continuous kinematic model for robot manipulators. IEEE Trans. Robot. Autom. 8 (4), 451–463.